Sol–gel synthesis and green luminescence of nanocrystalline Zn$_2$SiO$_4$:Mn phosphor

M. S. KWON*, C. J. KIM
Department of Materials Science and Engineering, University of Seoul, 90 Jeonnong-dong, Dongdaemun-gu, Seoul 130-743, South Korea
E-mail: mskwon@uos.ac.kr

H. L. PARK
Institute of Physics and Applied Physics, Yonsei University, Seoul 120-749, South Korea

T. W. KIM
Advanced Semiconductor Research Center, Division of Electrical and Computer Engineering, Hanyang University, Seoul 133-791, South Korea

H. S. LEE
Department of Materials Science and Metallurgy, Kyungpook National University, Daegu 702-701, South Korea

Zn$_2$SiO$_4$:Mn has been used as an efficient green-emitting phosphor for lamps and cathode ray tube screens [1, 2], which can be employed for plasma display panels (PDP), field emission displays (FED), backlight of liquid crystal displays (LCD) and electroluminescene (EL) devices due to high luminescent efficiency and chemical stability [1–6]. The particle size of most commercial phosphor materials prepared by traditional high-temperature solid-state reaction is over a micron size, thus the grains must be ground or milled to obtain fine power. The efficiency of the phosphor decreases greatly in those processes due to the damaged surfaces, and the morphology of the particle is changed unexpectedly. Also a high degree of compositional uniformity is hard to be achieved by high-temperature solid-state reaction. Sol–gel process is a very flexible low-temperature process to synthesize nanosized materials [7], which is easy to control the desired composition and to obtain a high degree of uniformity. In recent years, optical properties of nanosized phosphors have been studied extensively, and the nanosized phosphors have been known to behave differently from bulk phosphors of micron-size [3, 8–9].

In this letter, we report a novel sol–gel process to synthesize nanosized Zn$_2$SiO$_4$:Mn phosphor and its luminescent properties. We simply used ethanol as solvent and zinc acetate dihydrate, tetraethoxysilane, and Mn chloride tetrahydrate as starting materials to achieve a low-cost sol–gel route and to use simple and safe chemistry. Also all the processes were performed in a simple air environment without any further reducing heat treatments.

A stoichiometric amount of Zn(CH$_3$COO)$_2$·2H$_2$O and tetraethoxysilane (TEOS), was dissolved in ethanol, and then stirred for 30 min at room temperature. The stoichiometric amount means that the input ratio of Zn cation to Si cation was adjusted to 2:1 for Zn$_2$SiO$_4$ host materials. Then MnCl$_2$·4H$_2$O was added into the solution and stirred for 30 min again. The Mn composition was controlled by initial mol% with respect to the total moles of Zn and Si. Finally, NH$_4$OH was added into the solution to adjust the initial pH of the solution for 11. For pH 3, CH$_3$COOH was employed instead. The final solution was dried at 120 °C in air for 15 hr, transformed into dried amorphous gel powders. The obtained gel powder was finally calcined in air atmosphere at 1000 °C for 1 hr to induce crystallization of dried gel powder. X-ray diffraction (XRD) was used to identify the crystalline phases of sol–gel synthesized Zn$_2$SiO$_4$:Mn phosphors and to calculate the particle sizes according to Scherrer's formula [10]. Photoluminescence measurements were carried out with Hitachi F-4500 fluorescence spectrometer with a 150 W monochromatized Xe lamp using an excitation wavelength of 254 nm and a 430 nm cut-off to eliminate harmonic or scattering peaks.

Fig. 1 shows the XRD patterns of the sol–gel derived Mn-doped Zn$_2$SiO$_4$ phosphors prepared from the different initial pH conditions of initial solutions. For the purpose of comparison, Mn concentraion was fixed to an identical value, i.e., 2%. Fig. 1 shows the strong dependency of the formation of single crystalline phase Zn$_2$SiO$_4$ upon the initial pH condition of the solution. At pH 7, strong evidence of residual ZnO phase can be seen in Fig. 1. The residual peaks agree well with the standard pattern of ZnO of JCPDS card No. 36-1451 (space group number 186). At pH 3, it was found that the formation of ZnO residual phase was suppressed as seen in Fig. 1 though residual ZnO phase still existed. However, at pH 11, the formation of ZnO was suppressed completely and the single phase of crystalline Zn$_2$SiO$_4$ was obtained. At pH 11, all diffraction peaks can be assigned to Willemite (JCPDS card No. 37-1485, space group number 148). Thus, the control
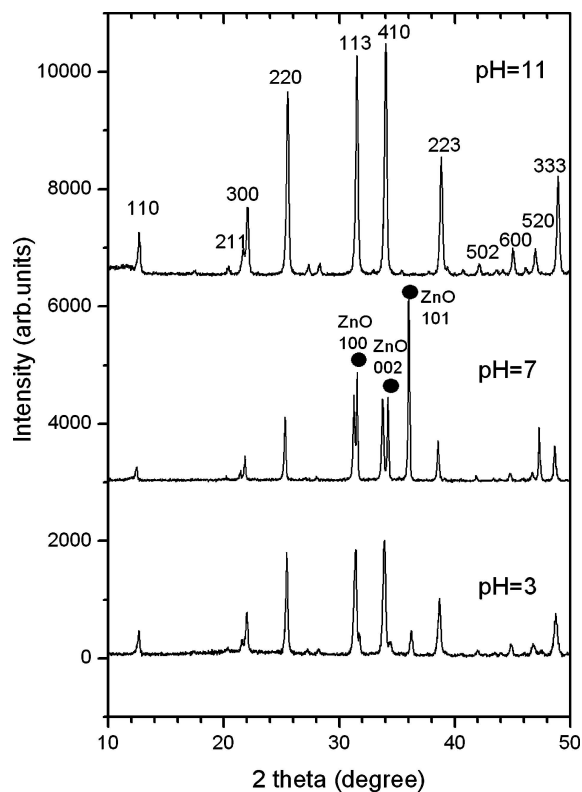
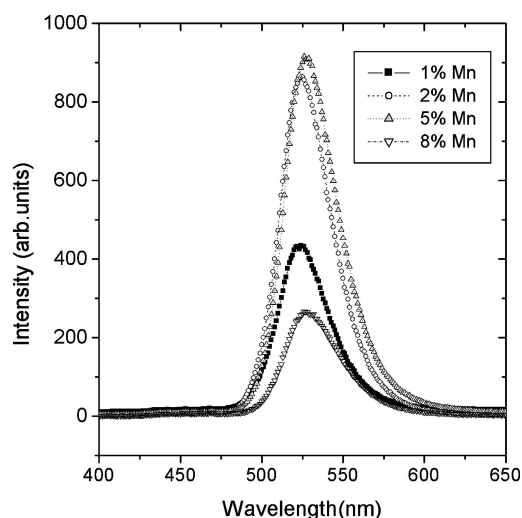*Figure 1* XRD patterns of nanosized Zn_2SiO_4:Mn phosphor from various initial pH conditions prepared by a sol–gel process.

Figure 2 Emission spectra of nanosized Zn_2SiO_4:Mn phosphor excited by 254 nm.

of initial pH condition is critical to obtain the single phase of Zn_2SiO_4 and the single phase can be obtained at pH 11 condition in this sol–gel process rather than pH 3 and pH 7 conditions.

Table I shows the calculated particle sizes according to Scherrer's formula [10], taking into account for the line broadening of diffracted peak due to the parti-

TABLE I Calibrated full width at half-maximum (FWHM) of the line broadening due to the particle-size effect alone and the calculated particle sizes of the Zn_2SiO_4:Mn phosphors synthesized by sol–gel process

Initial pH	3	7	11
FWHM (degree)	0.184	0.208	0.120
Particle size (nm)	46	87	41

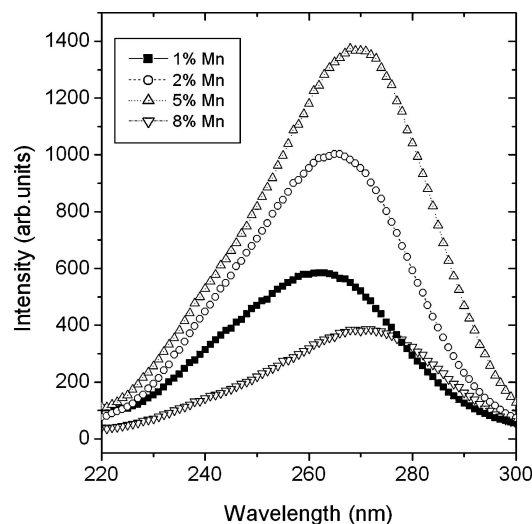*Figure 3* Excitation spectra of nanosized Zn_2SiO_4:Mn phosphor (emission wavelength monitored is 524 nm).

cle size effect alone. The maximum size measurable by line broadening is known to be almost 200 nm with the diffractometer [10]. We have used Warren's method [10] to determine the inherent line broadening from the diffractometer itself by using well-known Y_2O_2S:Eu commercial phosphor of micron-size. Table I shows that our sol–gel process produced the nanosized Zn_2SiO_4:Mn phosphors at the final calcining temperature of 1000 °C. Also, acid catalyst and base catalyst are found to have an effect on reducing the final crystalline particle sizes in our sol–gel process.

Fig. 2 shows the green emission spectra of sol–gel drived Zn_2SiO_4:Mn phosphors excited by 254 nm with the different Mn concentrations. We chose the initial pH condition as 11, considering that the final powder consisted of single-phase Zn_2SiO_4 under that condition, free from residual ZnO phase. The green emission spectra in Fig. 2 agree well with the literature value which has been assigned to an electronic transition of $^4T_1(^4G) \rightarrow {}^6A_1(^6S)$ peaking around the wavelength 525 nm and which is a parity forbidden emission transition of Mn^{2+} ions [4, 11]. Fig. 2 shows that the relative green emission intensity is increased with increasing of the Mn concentration upto 1%, 2%, and 5%. Then, for 8% of Mn, the relative emission intensity decreases, which shows a concentration-quenching phenomenon. Each emission spectra shows a maximum intensity at 524, 525, 526, 526 nm for 1%, 2% 5%, 8% Mn, respectively, which suggest a slight red-shift in emission spectra with increasing Mn concentration.

Fig. 3 shows the excitation spectra of the same Zn_2SiO_4:Mn phosphors measured for 524 nm emission in Fig. 2. Each excitation spectrum shows an excitation band ranging from 220 to 300 nm with a maximum around 263 nm, which mainly corresponds to charge transfer transition (or the ionization of manganese) from the divalent manganese ground state (Mn^{2+}) to the conduction band (CB) [11]. The tendency of excitation intensity is similar to that of emission as seen in Fig. 2, thus the most efficient excitation of charge transfer leads to the maximum emission intensity. The maximum excitation count appear at 263, 265.5, 268, 272 nm for 1%, 2%, 5%, 8% Mn, respectively, which
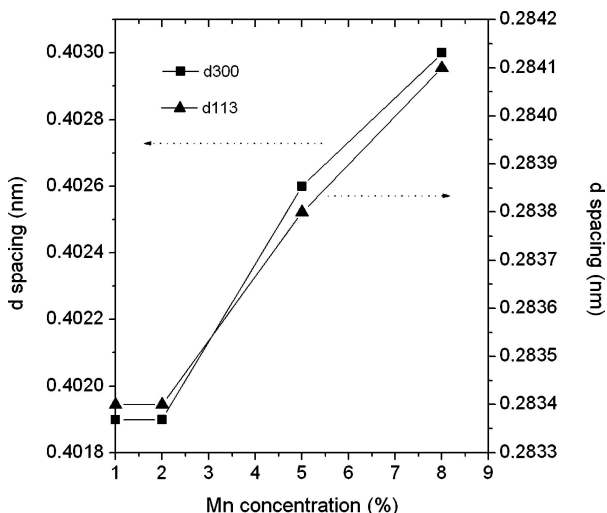
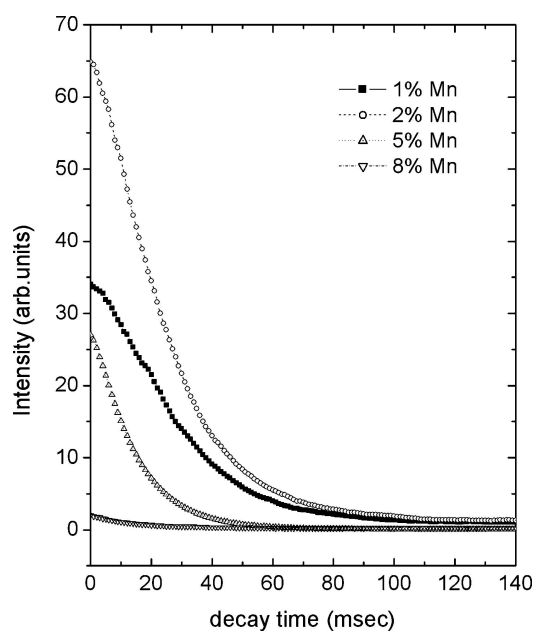*Figure 4* Changes of lattice spacings as a function of Mn concentration.

Figure 5 Photoluminescene decay curves of Zn_2SiO_4:Mn phosphors with different Mn concentrations.

shows a red-shift tendency with increasing the Mn concentration.

Fig. 4 shows the changes of lattice spacings of (300) and (113) atomic planes. (300) d-spacing corresponds to the changes of a-axis. (113) d-spacing relates the variations due to both a-axis and c-axis directions. It can be seen in Fig. 4, lattice spacings increase with increasing Mn concentration upto 8% in this experiment. Thus, the lattice strain effects, especially prominent in nanosized materials, may cause the red-shift tendency of emission and excitation with increasing Mn concentration.

Fig. 5 shows the photoluminescence decay curve of sol–gel synthesized Zn_2SiO_4:Mn phosphor as a func-

tion of Mn concentration under the initial pH 11 condition. The decay curves present phosphorescene life times. We simply measured the decay time, T, at the position of which intensity decreased by 1/e of the initial intensity. The decay time was 33, 28, 16, 19 ms for 1%, 2%, 5%, 8% Mn samples, respectively. The orders of decay times are in agreement with the previous observations [4, 6, 11, 12]. However, the shortest decay time was obtained for the sample of 5% Mn showing the highest emission intensity. Therefore, our sol–gel process showed a possibility that the decay time can be reduced via the control of Mn concentration with optimizing the emission intensity.

The sol–gel process derived in this letter offers a novel method to obtain nanosized Zn_2SiO_4:Mn green-emitting phosphor with compatible luminescence properties even at low temperatures for much shorter calcination times without needing any additional reducing environment compared to the traditional solid-state reaction for micron-size phosphors. The initial pH condition is important to obtain a single phase host materials. The green emission intensity of sol–gel derived Zn_2SiO_4:Mn green-emitting phosphor and the decay time can be optimized via the control of Mn concentration.

References
1. G. BLASSE and B. C. GRABMAIER, "Luminescent Materials" (Springer-Verlag, Berlin, 1994) p. 143.
2. S. SHIONOYA and W. M. YEN, "Phosphor Handbook," (CRC Press, Boston, 1999) Vol. 2, p. 469.
3. T. S. COPELAND, B. I. LEE, J. QI and A. K. ELROD, *J. Luminescence* **97** (2002) 168.
4. V. B. BHATKAR, S. K. OMANWAR and S. V. MOHARIL, *Phys. Stat. Sol. (a)* **191** (2002) 272.
5. Q. Y. ZHANG, K. PITA and C. H. KAM, *J. Phys.Chem. Mater.* **64** (2003) 333.
6. J. LIN, D. U. SANGER, M. MENNIG and K. BARNER, *Mat. Sci. Eng. B.* **64** (1999) 73.
7. A. S. EDELSTEIN and R. C. CAMMARATA, "Nanomaterials: Synthesis, Properties and Applications" (Institute of Physics Publishing, Bristol and Philadelphia, 1996) p. 145.
8. R. N. BHARGAVA, *J. Luminescence* **70** (1996) 85.
9. B. M. TISSUE, *Chem. Mater.* **10** (1998) 2837.
10. B. D. CULLITY, "Elements of X-ray Diffraction" (Addison-Wesley, Reading, Massachusetts, 1978) p. 284.
11. R. SELOMULYA, S. SKI, K. PITA, C. H. KAM, Q. Y. ZHANG and S. BUDDHUDU, *Mat. Sci. Eng. B.* **100** (2003) 136
12. S. SHIONOYA and W. M. YEN, "Phosphor Handbook," (CRC Press, Boston, 1999) Vol. 1, p. 170.